

Time-Stepping Numerical Simulation of Switched Circuits Within the Nonsmooth Dynamical Systems Approach

Vincent Acary, Olivier Bonnefon, and Bernard Brogliato

Abstract—The numerical integration of switching circuits is known to be a tough issue when the number of switches is large, or when sliding modes exist. Then, classical analog simulators may behave poorly, or even fail. In this paper, it is shown on two examples that the nonsmooth dynamical systems (NSDS) approach, which is made of: 1) a specific modeling of the piecewise-linear electronic devices (ideal diodes, Zener diodes, transistors); 2) the Moreau’s time-stepping scheme; and 3) specific iterative one-step solvers, supersedes simulators of the simulation program with integrated circuit emphasis (SPICE) family and hybrid simulators. An academic example constructed in [Maffezzoni, et al., IEEE Trans. CADICS, vol 25, no. 11, Nov. 2006], so that the Newton–Raphson scheme does not converge, and the buck converter are used to make extensive comparisons between the NSDS method and other methods of the SPICE family and a hybrid-like method. The NSDS method, implemented in the SICONOS platform developed at INRIA, proves to be on these two examples much faster and more robust with respect to the model parameter variations.

Index Terms—Analog simulation, backward Euler algorithm, complementarity dynamical systems, complementarity problems, multivalued systems, power converters, switching circuits, unilateral state constraints.

I. INTRODUCTION

IT IS WELL known that conventional accurate analog simulation tools, which are based on the Newton–Raphson nonlinear solver, can have serious drawbacks when they are used for the integration of nonsmooth circuits, containing switches and piecewise linear components (like ideal diodes and transistors). This is especially true when the number of events becomes too large, or when sliding modes exist, which is common in practice. Then, analog (SPICE-like) tools may become very time-consuming, or provide very poor results with chattering [28], or even fail [15], [18], [36], [37], [51]. The same applies to “hybrid” integrators that consider an exhaustive enumeration of all the system’s modes, which have a very limited scope of application because of the exponential growth of the number of modes that have to be simulated

separately. Along the same lines, event-driven schemes can hardly simulate systems with a large number of events because they soon become quite time-consuming and do not allow for accumulations of events [4].

It is, therefore, clear that other types of numerical schemes have to be applied for highly nonsmooth switching circuits. Since a numerical method always relies on a specific modeling approach, a logical path is to first reconsider the models of nonsmooth components (diodes, switches, transistors, etc.) so that efficient numerical solvers can be applied. The nonsmooth dynamical systems (NSDS) approach, which is the one chosen in this paper, appears to be a suitable framework for the simulation of nonsmooth circuits, allowing one to efficiently simulate systems with a very large number of events, and sliding mode trajectories. It consists of modeling nonsmooth components as piecewise-linear functions, with possible vertical branches (inducing some unilaterality in the system, hence possible state jumps, when these branches are infinite). The time discretization of such nonsmooth systems then yields various types of so-called one-step nonsmooth problems (OSNSP), for instance (linear) complementarity problems or nonlinear (or quadratic) programs with equality–inequality constraints. The NSDS approach may then take advantage of the quite important works that have been led by the Non-linear Programming community concerning the development of efficient solvers for complementarity problems [25] and optimization tools [31], and also by the Contact Mechanics community [4], where Moreau and Jean developed the so-called nonsmooth contact dynamics (NSCD) method within the theoretical framework of Moreau’s sweeping process [32], [41], [42]. The numerical method that is used in this paper, owes a lot to the NSCD method of mechanics, and will be named *Moreau’s time-stepping scheme*. As alluded to above, nonsmooth components are often represented with piecewise-linear functions, or with complementarity relations, or with inclusions into normal cones. The piecewise-linear modeling approach in nonsmooth electrical circuits has been pioneered by Chua *et al.* [33], and complementarity problems have been introduced in [45], [46], and [47], followed by the works of Leenaerts and van Bokhoven [34], [35], Vlach *et al.* [49], [50]. Camlibel *et al.* [16], [26] studied the convergence of backward Euler methods, and comparisons with other (analog and hybrid) integrators are proposed in [48]. Glocker *et al.* [29], [38] led interesting developments showing the analogy between

Manuscript received July 15, 2009; revised December 16, 2009. Date of current version June 18, 2010. The work of O. Bonnefon was supported by the Agence Nationale de la Recherche Project VAL-AMS, under Grant ANR-06-SETI-018-01. This paper was recommended by Associate Editor F. N. Najm.

The authors are with INRIA Grenoble Rhône-Alpes, St. Ismier Cedex 38334, France (e-mail: vincent.acary@inria.fr; bernard.brogliato@inria.fr; olivier.bonnefon@inria.fr).

Digital Object Identifier 10.1109/TCAD.2010.2049134

mechanics and electricity for various types of nonsmooth components, and also proposed a time-stepping method inspired by Moreau's algorithm for contact mechanics (consequently quite close to the algorithm used in this paper). Variational inequalities of the second kind and electrical superpotentials were recently introduced in electronics in [9], [10], and [30] to study the existence and uniqueness of solutions for static circuits, or the equilibria of dynamical circuits with nonsmooth devices. Other works may be found in [13] and [24].

The objective of this paper is twofold: firstly, it is shown on academic example taken from [36] that the NSDS approach allows one to simulate a nonsmooth system for which conventional analog methods fail (roughly speaking, the iterative solver for complementarity problems converges, whereas Newton–Raphson's method does not); secondly, numerical results for a buck converter are presented and comparisons with other (analog and hybrid) tools are done. The buck converter example in fact demonstrates on a significant case study that the proposed time-stepping method is efficient for systems with a large number of events. Compared to previous works [29], [48], the ideal switches are here modeled and simulated for the first time in a completely implicit way, the advantage of which will be explained. The simulations are done with the SICONOS software platform¹ of the INRIA [4], [7], [8], which is an open-source software package dedicated to nonsmooth dynamical systems.

This paper is organized as follows. In Section II, the modeling and general time discretization frameworks are recalled. In Section III, an elementary closed-loop switching circuit taken from [36] is simulated. In Section IV, an example exhibiting a sliding mode is studied. In Section V, the buck converter example is treated and comparisons are presented. Conclusion ends the paper.

Notation. The following tools will be used in this paper. Let $K \subseteq \mathbb{R}^n$ be a nonempty convex set. The normal cone to K at $x \in K$ is $N_K(x) = \{z \in \mathbb{R}^n \mid \langle z, \zeta - x \rangle \leq 0 \text{ for all } \zeta \in K\}$. The most familiar example of normal cones is $N_{[a,b]}(x) \subset \mathbb{R}$, $x \in \mathbb{R}$, $-\infty < a \leq b < +\infty$ which for $x \in [a, b]$ is given by

$$N_{[a,b]}(x) = \begin{cases} \mathbb{R}^-, & x = a \\ 0, & x \in (a, b) \\ \mathbb{R}^+, & x = b. \end{cases} \quad (1)$$

Its graph is depicted in Fig. 1(a).

For the particular value $a = -1$ and $b = 1$, the following equivalence relation is satisfied

$$y \in \text{sgn}(x) \Leftrightarrow x \in N_{[-1,1]}(y) \quad (2)$$

where the function $\text{sgn}(\cdot)$ is the multivalued signum function defined by

$$\text{sgn}(x) = \begin{cases} 1 & \text{if } x > 0 \\ -1 & \text{if } x < 0 \\ [-1, 1] & \text{if } x = 0 \end{cases} \quad (3)$$

and depicted in Fig. 1(b). Let us consider another very important case when one bound, say b , is equal to $+\infty$. We obtain

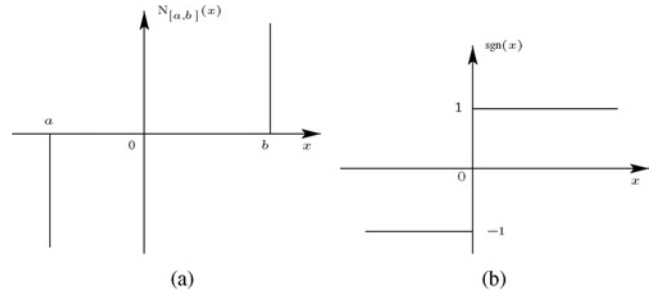


Fig. 1. Examples on familiar normal cones. (a) Normal cone $N_{a,b}(x)$. (b) Multivalued signum function.

$$N_{[a,+\infty)}(x) = \begin{cases} \mathbb{R}^-, & x = a, \\ 0, & x \in (a, +\infty). \end{cases} \quad (4)$$

This yields the so-called *complementarity condition*

$$-y \in N_{[a,+\infty)}(x) \Leftrightarrow 0 \leq x - a \perp y \geq 0 \quad (5)$$

where $x \perp y$ means that $x^T y = 0$. In the case of vectors $x, y \in \mathbb{R}^n$, the inequalities have to be understood component-wise.

The projection in the euclidean metric of a vector $x \in \mathbb{R}^n$ onto K is denoted as $\text{proj}[K; x]$. A singleton is denoted as $\{t\}$. The identity matrix of $\mathbb{R}^{m \times m}$ is denoted by I_m and the zero vector in \mathbb{R}^m by 0_m .

The following standard mathematical programming problems will be used throughout this paper.

Definition 1 (Variational Inequality [25]): Given a function $F: \mathbb{R}^p \rightarrow \mathbb{R}^p$, and Ω a nonempty subset of \mathbb{R}^p , the variational inequality (VI) problem is to find a vector $z \in \mathbb{R}^p$ such that

$$F^T(z)(y - z) \geq 0, \forall y \in \Omega. \quad (6)$$

□

Definition 2 (Inclusion into a Normal Cone [43]): Given a function $F: \mathbb{R}^p \rightarrow \mathbb{R}^p$, and K a nonempty convex subset of \mathbb{R}^p , the inclusion into a normal cone problem is to find a vector $z \in \mathbb{R}^p$ such that

$$0 \in F(z) + N_K(z). \quad (7)$$

□

If $K = \Omega$ is a convex set, the inclusion (7) and the VI (6) are equivalent.

Definition 3 (Mixed Complementarity Problem [22]): The mixed complementarity problem (MCP) is defined as follows. Given a function $F: \mathbb{R}^p \rightarrow \mathbb{R}^p$, lower and upper bounds $l, u \in (\mathbb{R} \cup \{+\infty, -\infty\})^p$, find $z \in \mathbb{R}^p$, $w, v \in \mathbb{R}_+^p$, such that

$$\begin{cases} F(z) = w - v \\ l \leq z \leq u, & (z - l)^T w = 0, & (u - z)^T v = 0. \end{cases} \quad (8)$$

□

Notice that a solution of the MCP satisfies the inclusion $-F(z) \in N_{[l,u]}(z)$. If $F(\cdot)$ in (8) is affine, which is

¹See <http://siconos.gforge.inria.fr/>.

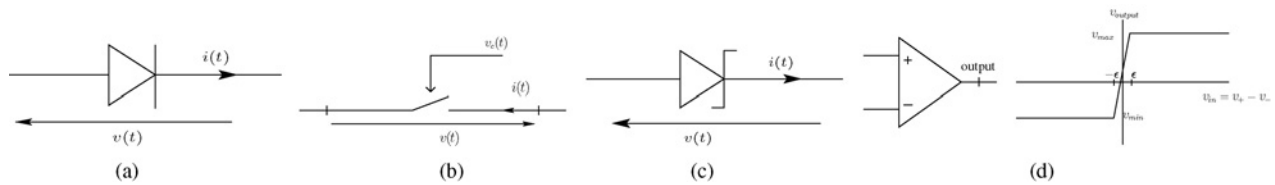


Fig. 2. Nonsmooth models. (a) Diode symbol. (b) Ideal switch symbol. (c) Zener diode symbol. (d) Comparator symbol and model.

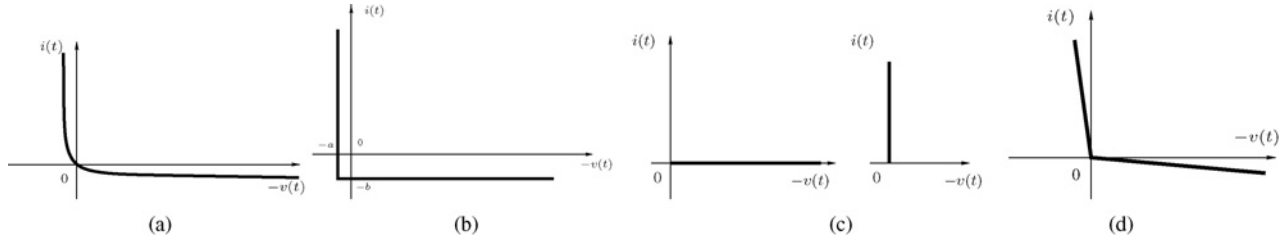


Fig. 3. Four models of diodes. (a) Smooth modeling. (b) Nonsmooth modeling. (c) Hybrid modeling. (d) Equivalent resistor model.

$$\begin{cases} Mz + q = w - v \\ l \leq z \leq u, \quad (z - l)^T w = 0, \quad (u - z)^T v = 0 \end{cases} \quad (9)$$

for some matrix $M \in \mathbb{R}^{p \times p}$ and some vector $q \in \mathbb{R}^p$, the MCP (8) defines a mixed linear complementarity problem (MLCP).

II. NSDS APPROACH

A. Nonsmooth Electronic Devices Modeling

The NSDS approach for the modeling of piecewise-linear components in electrical circuits has been described in detail in [4], [29], [32], [41], and [42], and will just be recalled here for the sake of readability. The NSDS approach is a package that consists of: 1) nonsmooth models; 2) Moreau's time-stepping algorithm; and 3) OSNSP solvers. The current-voltage laws of nonsmooth electronic devices may all be represented as inclusions into a normal cone to a convex set K , i.e., $0 \in \Phi(y, \lambda, t) + N_K(\lambda)$, where $\Phi(\cdot)$ is a function, y and λ are implicitly defined from $0 = H(X, \lambda, t)$ and $y = G(X, \lambda, t)$ for some functions $H(\cdot)$ and $G(\cdot)$. The state vector of the circuit X is composed of branch voltages and currents. A crucial point for simulation efficiency, however, is to keep as less slack variables, λ and y , as possible in the device representation. In addition, some efficient OSNSP solvers (as they will be described in Section II-D) use directly such inclusions into a normal cone to a convex set, or the equivalent VI formulation. This is the case for the direct MCP solvers that we used in our simulations. Finally, it is noteworthy that the inclusion modeling of the devices allows for nonlinear characteristics which may not be represented by complementarity relations.

Let us illustrate this on the above four examples (ideal diode, switch, transistor, and comparator).

1) *Nonsmooth Diodes*: The notation for the currents and the potentials at the ports of the diode is depicted in Fig. 2(a). Following four models of diodes are depicted in Fig. 3.

- 1) The smooth exponential Shockley model in Fig. 3(a) defined by the smooth constitutive equation

$$i = i_s (e^{\frac{v}{\alpha}} - 1) \quad (10)$$

where i_s and α are physical parameters of the diode.

- 2) Ideal diodes with possible residual current b and voltage a in Fig. 3(b) defined by the following complementarity condition

$$0 \leq i + b \perp a - v \geq 0 \iff -(i + b) \in N_{[-a, +\infty)}(-v). \quad (11)$$

- 3) The ‘‘hybrid’’ model, which considers the two modes separately with, for instance, an associated Modelica [23] script in Fig. 3(c)

$$\begin{aligned} \text{off} &= s < 0 \\ v &= \text{if off then } s \text{ else } 0 \\ i &= \text{if off then } 0 \text{ else } s. \end{aligned} \quad (12)$$

- 4) A piecewise-linear model in Fig. 3(d) defined by

$$v = \begin{cases} R_{\text{on}} i & \text{if } v < 0 \\ R_{\text{off}} i & \text{if } v \geq 0 \end{cases} \quad (13)$$

where $R_{\text{on}} \ll 1$ and $R_{\text{off}} \gg 1$ are the equivalent resistive values of each branch.

The ideal diode model in Fig. 3(b) is chosen in this paper. The drawback of the Shockley law is that it introduces high stiffness in the dynamical equations. The hybrid model becomes rapidly unusable if the number m of diodes increases, since the number of modes to be described in the associated script varies as 2^m . The model in Fig. 3(d) leads a badly conditioned algorithm used to solve the OSNSP in Section II-D. On the contrary, the ideal model of Fig. 3(b) yields, when introduced in the dynamics, well-conditioned complementarity problems, that yield time-stepping methods for which efficient solvers exist. Showing the efficiency of these methods is the object of this paper.

From basic convex analysis one deduces that the ideal diode of Fig. 3(b) has the following current/voltage law:

$$i \in \{-b\} + N_{]-\infty, a]}(v) \Leftrightarrow -v \in \{-a\} + N_{]-\infty, b]}(-i). \quad (14)$$

The piecewise-linear diode of Fig. 3(d) can be represented as

$$\begin{cases} v = \frac{1}{2}(1 + \tau)R_{\text{on}}i + \frac{1}{2}(1 - \tau)R_{\text{off}}i \\ \tau \in \text{sgn}(v) \Leftrightarrow v \in N_{[-1, 1]}(\tau) \end{cases} \quad (15)$$

that is consistent with the MLCP formulation in (9). The piecewise-linear model yields a condition number of the resulting MLCP matrix close to $R_{\text{off}}/R_{\text{on}}$, that causes trouble with the numerical algorithms that are used to solve the OSNSP. Inclusions as in (14) will be preferred as they can be directly used in the numerical algorithm for MCP, yielding well-posed and well-conditioned MCPs.

2) *Nonsmooth Switches*: The notation for the currents and the potentials at the ports of the ideal switch is depicted in Fig. 2(b). The switches are modeled in two ways in this paper. The first model, which is applied to the elementary example of Section III, consists of

$$v = \begin{cases} R_{\text{off}} i & \text{if } v_c < 0 \\ R_{\text{on}} i & \text{if } v_c \geq 0 \end{cases} \quad (16)$$

where the voltage v_c is a state variable of the overall dynamical system, v is the voltage of the switch and i is the current through the switch. The resistors $R_{\text{off}} \gg 1$ and $R_{\text{on}} \ll 1$ are chosen by the designer. In the case of the buck converter of Section V, the switch is modeled with transistors, as is most common in the industrial practice. The switch in (16) is modeled as follows:

$$\begin{cases} v = \frac{1}{2}(1 + \tau)R_{\text{on}}i + \frac{1}{2}(1 - \tau)R_{\text{off}}i \\ \tau \in \text{sgn}(v_c) \Leftrightarrow v_c \in N_{[-1, 1]}(\tau) \end{cases} \quad (17)$$

which is equivalent to the 4-mode disjunctive formulation

$$\begin{cases} \text{if } v_c < 0 & \text{then } \tau = -1 & \text{and } v = R_{\text{off}}i \\ \text{if } v_c > 0 & \text{then } \tau = 1 & \text{and } v = R_{\text{on}}i \\ \text{if } v_c = 0, i \geq 0 & \text{then } \tau \in [-1, 1] & \text{and } v \in [R_{\text{on}}i, R_{\text{off}}i] \\ \text{if } v_c = 0, i < 0 & \text{then } \tau \in [-1, 1] & \text{and } v \in [R_{\text{off}}i, R_{\text{on}}i]. \end{cases} \quad (18)$$

The difference with respect to the diode (15) is that the ‘‘input’’ to the inclusion is an external voltage. It is noteworthy that the voltage v in (16) is discontinuous at $v_c = 0$ for any $i \neq 0$, the jump magnitude being equal to $|(R_{\text{off}} - R_{\text{on}})i|$. The choice that is made in (17) implies that the discontinuities are ‘‘filled-in’’ and the model is consequently multivalued at $v_c = 0$, $i \neq 0$. This is precisely what allows one to smoothly simulate the sliding modes [5].

The proposed model (17) is not a real ideal switch because when the switch is open, there is still a resistor in operation if $R_{\text{on}} \neq 0$. There is no trouble in using $R_{\text{on}} = 0$ to obtain a real ideal switch in open operation mode. In the sequel, the value of R_{on} is different from 0 and this choice is motivated by the industrial practice and the way switches are modeled in Mentor Graphics’ ELDO software package,² which is one

²See http://www.mentor.com/products/ic_nanometer_design/analog-mixed-signal-verification/eldo/.

of the main analog simulation tool of the market and may be considered as a reference for simulation results comparisons.

Remark 1: The ideal switch is modeled in [29] with a relay multifunction whose threshold may vary between 0 and $+\infty$, and the switch is controlled by a current variable of the circuit, in an explicit way. Compared to [48] our approach differs a lot since [48] models the switch through a so-called cone complementarity problem, with an exogenous excitation that makes the cones $[\Omega$ in (6) or K in (7)] switch between $\{0\}$ and \mathbb{R} or \mathbb{R}^+ . Another way to model switches is to compute the topology changes after each ‘‘open’’ and ‘‘close’’ operation. As pointed out above such an approach rapidly becomes extremely time-consuming when the number of switches grows (the number of different topologies grows exponentially fast with the number of switches), and does not allow for finite accumulations of switches or sliding mode trajectories. An open issue is the implicit discretization of the ideal switches models of [29] and [48] that is not directly possible and is not tackled in this paper.

3) *Nonsmooth Zener Diodes*: Similar inclusions for ideal Zener diodes may be found in [4] and [10], that take the form $-i \in N_{[0, v_z]}(-v)$ for some $v_z > 0$ with the convention illustrated in Fig. 2(c).

4) *Nonsmooth Comparator*: The comparator device as depicted in Fig. 2(d) is modeled as a piecewise-linear function whose value is v_{min} if $x < -\epsilon V$, $v_{\text{min}} + (v_{\text{max}} - v_{\text{min}})(x + \epsilon)/(2\epsilon)$ if $-\epsilon V < x < \epsilon V$ and v_{max} if $x > \epsilon V$. Setting ϵ to 0 leads to a relay function that is multivalued at 0. In this case, similarly to the Zener diode the multivalued comparator is represented as

$$v_+ - v_- \in N_{[v_{\text{min}}, v_{\text{max}}]}(v_{\text{output}}) \quad (19)$$

where v_{min} and v_{max} are the saturation thresholds.

B. Dynamical Equations

Section II-A is devoted to present the electronic devices models and their mathematical representations to be inserted in the circuit dynamics in order to obtain a suitable formalism for the subsequent time discretization. In particular, the OSNSP solver to be used strongly influences the modeling choice. In this section, we focus on the dynamical equations that are suitable for the NSDS approach.

1) *Nonsmooth Differential Algebraic Equations (DAE) Formulation*: The circuit with nonsmooth components represented as inclusions and equalities, and the smooth nonlinear behavior of the network represented as DAE can be written compactly as

$$\begin{cases} M(X, t)\dot{X} = F(X, t) + U(t) & \text{DAE} \\ \begin{cases} 0 = H(X, \lambda, t) \\ y = G(X, \lambda, t) \end{cases} & \text{Input/output relations on} \\ & \text{nonsmooth components} \\ 0 \in \Phi(y, \lambda, t) + N_K(\lambda) & \text{‘‘Inclusion rule’’} \end{cases} \quad (20)$$

where $X \in \mathbb{R}^n$ is the state composed of the potentials and the currents in inductive, voltage-defined and nonsmooth branches. The vectors $y, \lambda \in \mathbb{R}^m$ are the slack variables

for a given ζ^0 . At each time-step k and at each Newton iteration α , the problem (26) appears to be affine in ζ .

D. Numerical Solvers for the OSNSP (22)

The problem (22) is a VI written in the form of an inclusion into a normal cone to a convex set as in (23). The choice of the numerical solver for (22) depends mainly on the structure of the convex set K . Indeed, from a very general convex set K to a particular choice of K , the numerical solvers range from the numerical methods for VI to nonlinear equations, passing through various complementarity problem solvers. The convergence and the numerical efficiency are improved in proportion as the structure of K becomes simpler. In the sequel, majors choices of K will be given leading to various classes of well-known problems in mathematical programming theory. We refer to [25] for a thorough presentation of available numerical solvers and to [4, Ch. 12] for a comprehensive summary of numerical algorithms. In the numerical examples presented in this paper, various numerical methods described below are used according to the type of the OSNSP and will be further precised.

1) *K is a Finite Representable Convex Set:* In practice, the convex set is finitely represented by

$$K = \{\lambda \in \mathbb{R}^m \mid h(\lambda) = 0, g(\lambda) \geq 0\} \quad (27)$$

where the functions $h: \mathbb{R}^m \rightarrow \mathbb{R}^m$, $g: \mathbb{R}^m \rightarrow \mathbb{R}^m$ are assumed to be smooth with nonvanishing Jacobians. More precisely, we assume that the following constraints qualification holds:

$$\forall \lambda \in K, \exists d \in \mathbb{R}^m, \text{ such that } \begin{cases} \nabla^T h_i(\lambda)d < 0, i = 1 \dots m \\ \nabla^T g_j(\lambda)d < 0, j \in \mathcal{I}(\lambda) \end{cases} \quad (28)$$

where $\mathcal{I}(\lambda)$ is the set of active constraints at λ , which is

$$\mathcal{I}(\lambda) = \{j \in 1 \dots m, g_j(\lambda) = 0\}. \quad (29)$$

In this case, general algorithms for VI can be used. To cite a few, the minimization of the so-called regularized gap function [27], [52], [53] or generalized Newton methods [25, Chs. 7 and 8] can be used. If $F(\cdot)$ is affine [possibly after the linearization step described in (26)] and the functions $h(\cdot)$ and $g(\cdot)$ are also affine, the VI is said to be an affine VI for which the standard pivoting algorithms for linear complementarity problem (LCP) [19] are extended in [17].

2) *K is a Generalized Box:* Let us consider the case that K is a generalized box that is

$$K = \{\lambda \in \mathbb{R}^m \mid a_i \leq \lambda_i \leq b_i, a_i \in \overline{\mathbb{R}}, b_i \in \overline{\mathbb{R}}, i = 1 \dots m\} \quad (30)$$

with $\overline{\mathbb{R}} = \{\mathbb{R} \cup \{+\infty, -\infty\}\}$. In this case, the problem (23-25) can be recast into a mixed complementarity problem (MCP) by defining $p = n + m + m + m$ and the bounds l, u as $l = [0_n \ 0_m \ 0_m \ a]^T$ and $u = [0_n \ 0_m \ 0_m \ b]^T$.

The MCP (8) can be solved by a large family of solvers based on Newton-type methods and interior-points techniques. In contrast to the interior-point methods, it is not difficult to find comparisons of numerical methods based on Newton's method for solving MCPs. We refer to [14] for an impressive comparison of the major classes of algorithms for solving MCPs. If $F(\cdot)$ is affine, the MLCP is equivalent to a box-constrained affine VI. For this problem, the standard pivoting algorithm such the Lemke's method is extended in [44]. A special case of a generalized box is the positive orthant of \mathbb{R}^m , which is $K = \mathbb{R}_+^m$. Standard theory and most of the numerical algorithms for LCPs apply in this MCLP case.

When the circuit is simple and of low size in terms of the number of state variables, it is sometimes possible to write the DAE as an ordinary differential equation (ODE) and perform the explicit substitution of X by y and λ in the formulation (22). If the cone is also simply defined by a positive orthant, we arrive then at a standard LCP [21]. Unfortunately, the LCP formulation is not amenable for more complicated cases where an automatic circuit equation formulation is used.

E. Specificities of Moreau's Time-Stepping Method for Circuits in the Form (21)

In this section, we give more details on the specificities of the time integration with the Moreau scheme. Let us assume that the solution in the unknowns x, z is sought depending on the following cases.

- 1) *Absolutely continuous solution case:* In this case, the function $x(\cdot)$ (respectively $z(\cdot)$) is assumed to be an absolutely continuous function of time. More precisely, its time-derivative $\dot{x}(\cdot)$ (respectively $\dot{z}(\cdot)$) is a right continuous function of bounded variations in time such that

$$x(t) = x(t_0) + \int_{t_0}^t \dot{x}(s) ds \quad (31)$$

and $\dot{x}(t) = \dot{x}^+(t) = \lim_{s \rightarrow t, s > t} \dot{x}(s)$ (respectively for $z(\cdot)$). By consistency, the function $\lambda(\cdot)$ (respectively $y(\cdot)$) is a right-continuous function of bounded variations in time.

- 2) *Bounded variation solution case:* The unknown state vector $x(\cdot)$ (respectively $z(\cdot)$) is assumed to be a function of bounded variations in time. The time derivative of $x(\cdot)$ cannot be defined as a standard time-derivative but as a differential measure dx that can contain a Dirac measure. In the same way, $z(\cdot), y(\cdot)$ are functions of bounded variations and the multiplier λ is replaced by $d\lambda$, which is also a measure. This case happens when the initial conditions are not consistent and/or some jumps are encountered due to inconsistent unknown vector with unilateral constraints imposed by the inclusion.

Naturally, the above observations are slightly abusive and need a rigorous mathematical framework, which is beyond the scope of this paper. Nevertheless, we can cite the pioneering work of Moreau on such subjects [39], [40] and its extension [6] where the notion of relative degree plays a fundamental role in the nature of solutions and therefore in the specificities of the time integration.

With the previous assumption on the (low) regularity on the solution, several precautions have to be taken by the time discretization. These precautions together with the mathematical framework introduced by Moreau are at the heart of the approach. Let us explain the simplest case of an absolutely continuous solution $x(\cdot)$. The derivative $\dot{x}(\cdot)$, which is of bounded variations, is estimated by a rough backward Euler scheme

$$h\dot{x}(t_{k+1}) \approx x_{k+1} - x_k. \quad (32)$$

Note that a higher order approximation is a nonsense due to the nonsmoothness of $\dot{x}(\cdot)$. The functions of bounded variations λ and y are estimated in a fully implicit way to satisfy the inclusion rule at t_{k+1} , which is

$$\begin{cases} y = g(x, z, \lambda) \\ -y \in N_K(\lambda) \end{cases} \approx \begin{cases} y_{k+1} = g(x_{k+1}, z_{k+1}, \lambda_{k+1}), \\ -y_{k+1} \in N_K(\lambda_{k+1}). \end{cases} \quad (33)$$

This fact is crucial to ensure the convergence of the scheme and a chattering-free discrete solution when a constraint remains active. For the remaining part of the system (21), if the regularity is sufficient we can choose a θ -method with $\theta \in [0, 1]$. The fully implicit case $\theta = 1$ ensures the stability for the stiff nonlinear terms and the fully explicit case $\theta = 0$ ensures the efficiency in terms of CPU effort if the system is nonstiff. A part of the stiff nonlinearity can be included in the inclusion form and mildly nonlinear systems can be obtained.

All these remarks lead to the following integration scheme for the original system (21):

$$\begin{cases} x_{k+1} - x_k = hf_1(x_{k+\theta}, z_{k+\theta}, t_{k+1}) + hU(t_{k+\theta}) \\ 0 = f_2(x_{k+1}, z_{k+1}, t_{k+1}) \\ 0 = h(x_{k+1}, z_{k+1}, \lambda_{k+1}, t_{k+1}) \\ y = g(x_{k+1}, z_{k+1}, \lambda_{k+1}, t_{k+1}) \\ 0 \in \Phi(y_{k+1}, \lambda_{k+1}, t_{k+1}) + N_K(\lambda_{k+1}). \end{cases} \quad (34)$$

The case of bounded variation is written in terms of the difference $x_{k+1} - x_k$ and the approximation of the measure of the time interval is $p_{k+1} = hd\lambda((t_k, t_{k+1}])$. The value p_{k+1} is homogeneous to an impulse of value $h\lambda_{k+1}$. This is the only way to ensure the consistency of the scheme at jumps because the value of λ_{k+1} goes to infinity when the time-step h goes to zero. Indeed, it reflects that the point-wise evaluation of a measure is a nonsense.

Finally, some works are done to design adaptive time-step strategies for the Moreau scheme. The absolutely continuous case can be treated by standard practical apparatus for the low order error estimations. In the case of bounded variations solutions, some care has to be taken. A flavor of possible solutions and open issues can be found for mechanical systems with impacts in [1].

F. Software Implementation

Finally, some insights are given on the software implementation of the methods. A Netlist is a circuit textual description used by many simulators such as SPICE and ELDO. From a Netlist, the automatic generator builds all the components defined in (21). The opensource SICONOS/KERNEL library performs the time discretization following the Moreau

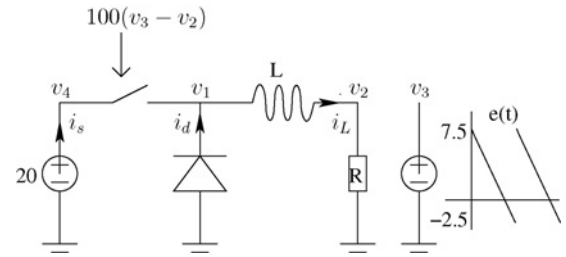


Fig. 4. Simple switched circuit.

time-stepping scheme (22) and formulates at each time-step one instance of the inclusion problem (23)–(25). The numerical algorithms for the latter problem are in the opensource SICONOS/NUMERICS library. The output of the simulation is a file containing the potential and current values in the SPICE format.

The implementation is object-oriented and mainly in C++. For each electrical component, group of equations and inclusions in (22), a corresponding instance of a class is built. The system is updated in memory at each iteration by the stamp method of each component. In the linear case, these methods are called only once, in the nonlinear case they may be called at any time to update the system. The open-source platform is under Gnu general public licence and can be freely used. The equation generator is under private license and can be obtained freely on demand for an academic use. Note that the actual implementation of the software does not exploit the inherent sparsity of the system. This is mainly due to development effort restriction. It is clear that substantial gain may be expected by using standard sparse library.

III. ELEMENTARY SWITCHING CIRCUIT

This section is devoted to the modeling and the simulation of the circuit in Fig. 4. In [36], it is shown that Newton–Raphson-based methods fail to converge on such a circuit, with the switch model as in (16). The diode model is the equivalent resistor model of Fig. 3(d). On the contrary, the OSNSP solver correctly behaves on the same model.

A. Dynamical System

The dynamics of the circuit in Fig. 4 is obtained using the algorithm of automatic circuit equation formulation. In a first step, the vector of unknowns is built; in a second step, the dynamical system is written; and in a last step, the nonsmooth laws are added. Applying the automatic equations generation algorithm leads to the following 9-D unknown (dynamic and algebraic unknown) vector: $X = (v_1 \ v_2 \ v_3 \ v_4 \ i_L \ i_{03} \ i_{04} \ i_s \ i_d)^T$ in the system (20) or $x = (i_L) \ z = (v_1 \ v_2 \ v_3 \ v_4 \ i_{03} \ i_{04} \ i_s \ i_d)^T$ in the system (21), where the potentials and the currents are depicted in Fig. 4. Building the dynamical equations consists in writing the Kirchhoff current laws at each node, the constitutive equation of the smooth branch, and the nonsmooth law of the other branches. The two nonsmooth devices are the diode and the switch. It yields the following system that fits within the general framework in (21): for the semi-explicit DAE, we obtain

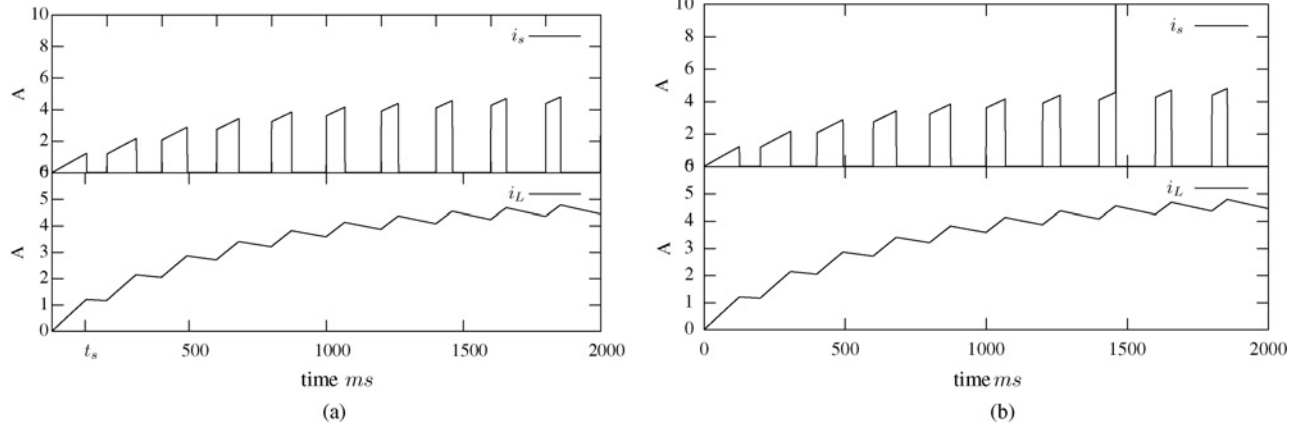


Fig. 5. Switched circuit simulations. (a) SICONOS simulation. (b) ELDO simulation.

$$\begin{cases} L \frac{di_L}{dt}(t) = v_1(t) - v_2(t) \\ i_d(t) + i_s(t) - i_L(t) = 0, & i_L(t) - \frac{v_2(t)}{R} = 0 \\ i_{03}(t) = 0, & i_{04}(t) - i_s(t) = 0 \\ v_4(t) = 20, & v_3 = e(t). \end{cases} \quad (35)$$

For the input/output relations on nonsmooth components, we get

$$\begin{cases} v_1(t) = \frac{1}{2}(\tau_1(t) - 1)R_{\text{off}}i_d(t) - \frac{1}{2}(\tau_1(t) + 1)R_{\text{on}}i_d(t) \\ 2(v_4(t) - v_1(t)) = [(1 + \tau_2(t))R_{\text{off}} + (1 - \tau_2(t))R_{\text{on}}]i_s(t). \end{cases} \quad (36)$$

Finally, the inclusion rule is written as

$$\begin{cases} v_1(t) \in -N_{[-1,1]}(\tau_1(t)) \\ 100(v_3(t) - v_2(t)) \in -N_{[-1,1]}(\tau_2(t)). \end{cases} \quad (37)$$

On this example, the fully implicit ($\theta = 1$) Moreau's scheme reads as

$$\begin{cases} L(i_{L,k+1} - i_L) = h(v_{1,k+1} - v_{2,k+1}) \\ i_{d,k+1} + i_{s,k+1} - i_{L,k+1} = 0, & i_{L,k+1} - \frac{1}{R}v_{2,k+1} = 0 \\ i_{03,k+1} = 0, & i_{04,k+1} - i_{s,k+1} = 0 \\ v_{4,k+1} = 20, & v_{3,k+1} = e(t_{k+1}) \\ 2v_{1,k+1} = (\tau_{1,k+1} - 1)R_{\text{off}}i_{d,k+1} - (\tau_{1,k+1} + 1)R_{\text{on}}i_{d,k+1} \\ 2(v_{4,k+1} - v_{1,k+1}) \\ = [(1 + \tau_{2,k+1})R_{\text{off}} + (1 - \tau_{2,k+1})R_{\text{on}}]i_{s,k+1} \\ v_{1,k+1} \in -N_{[-1,1]}(\tau_{1,k+1}) \\ 100(v_{3,k+1} - v_{2,k+1}) \in -N_{[-1,1]}(\tau_{2,k+1}). \end{cases} \quad (38)$$

B. Numerical Results With SICONOS

The time-step has been fixed to $0.1 \mu\text{s}$, the values of the parameters are $R = 1 \Omega$, $R_{\text{on}} = 0.001 \Omega$, $R_{\text{off}} = 1000 \Omega$, $L = 2 \cdot 10^{-4} \text{H}$, and the initial condition is $i_L(0) = 0 \text{A}$. Fig. 5(a) depicts the current evolution through the inductor L . In [36], it has been shown that the Newton–Raphson algorithm fails when the state of the diode and of the switch changes at $t = t_s$ in Fig. 5(a). Indeed, the linearization performed at each Newton–Raphson iteration leads to an oscillation between two

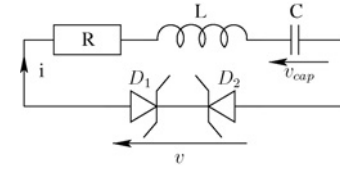


Fig. 6. RLC Zener diodes circuit.

incorrect states and never converges to the correct one. The Newton–Raphson iterations enter into a infinite loop without converging. Using the NSDS approach the OSNSP solver converges and computes the correct state. For such a simple system, any OSNSP solver gives a correct solution. We have used indifferently PATH and a semi-smooth Newton method.

Remark 2: In [36], an event-driven numerical method is proposed to solve the nonconvergence issue. However it is reliable only if the switching times can be precisely estimated, a shortcoming not encountered with the NSDS and the Moreau's time-stepping method.

C. Numerical Results With ELDO

ELDO does not provide any nonsmooth switch model. But it furnishes the “VSWITCH” one described in (39), where R_S is the controlled resistor value of the switch, and v_c the voltage control yielding to the model

$$R_S(t) = \begin{cases} R_{\text{on}} & \text{if } v_c(t) \geq v_{\text{on}} \\ R_{\text{off}} & \text{if } v_c(t) \leq v_{\text{off}} \\ (v_c(t)(R_{\text{off}} - R_{\text{on}}) + R_{\text{on}}v_{\text{off}} - R_{\text{off}}v_{\text{on}})/(v_{\text{off}} - v_{\text{on}}) & \text{otherwise} \end{cases} \quad (39)$$

setting v_{off} to 0, and choosing a small value for v_{on} lead to a model close to (16) for the chosen parameters.

Simulations have been done using different sets of parameters. It is noteworthy that the behavior of ELDO depends on these values. For example, using a Backward Euler with the time-step fixed to $0.1 \mu\text{s}$ and $v_{\text{on}} = 10^{-4} \text{V}$, $v_{\text{off}} = 0 \text{V}$, $R_{\text{off}} = 1000 \Omega$, $R_{\text{on}} = 0.001 \Omega$ causes trouble during the ELDO simulation: “Newton no-convergence” messages appear. Fig. 5(b) shows the ELDO simulation. The values are

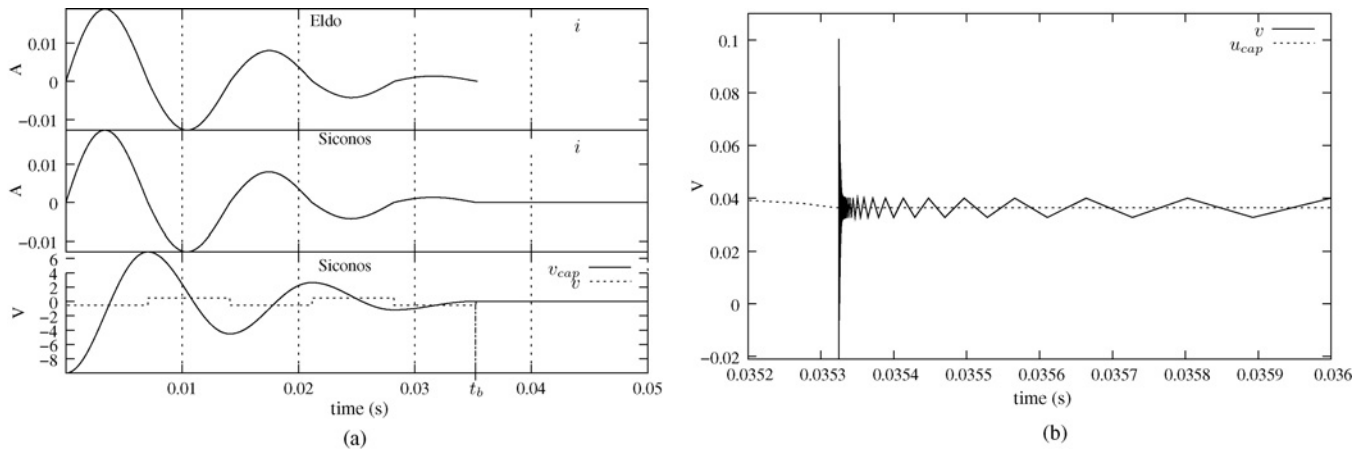


Fig. 7. Simulation of the circuit with sliding mode. (a) Nonsmooth model in SICONOS and hybrid model in VERILOG/ELDO simulation. (b) Regularized model in ELDO. Zoom in the neighborhood of the switching time.

very close to the SICONOS simulation, except for the steps corresponding to the “no-convergence” messages. In this case, the resulting current value is absurd.

This academic example demonstrates that analog tools can fail to simulate a switched circuit.

IV. EXAMPLE SHOWING A SLIDING MODE

The goal of this section is to focus on the very interesting feature of the nonsmooth approach: the possibility to simulate consistently multivalued components and then coherently ideal components. The point is not to show that ideal components are better for the physical modeling accuracy, but rather that the regularization or standard hybrid approaches are not convenient for a high-level description and design. Our goal is to show that it is better to have a right simulation with an ideal model rather than a simulation that does not work correctly with a regularized model and pseudo-physics.

Let us consider a multivalued component, more precisely, we choose a multivalued behavior of a couple of Zener diodes. The goal is to outline the efficiency of the nonsmooth model by inclusions to handle such a behavior, even when a sliding mode occurs. In this context, the sliding mode has to be understood as a mode whose operating point of the component is in the multivalued part. The circuit is depicted in Fig. 6.

A. Models and Dynamical Systems

The choice of the vector of unknowns is $[i, v_{cap}]^T$ and yields

$$L \frac{di(t)}{dt} = -Ri(t) - v_{cap}(t) + v(t), \quad C \frac{dv_{cap}(t)}{dt} = i(t). \quad (40)$$

1) Nonsmooth Model of Double Opposite Zener Diodes:

For simplicity's sake, the two Zener diodes D_1 and D_2 in Fig. 6 are modeled as a single component. The behavior of the whole component is given by

$$-i \in N_{[-v_z, v_z]}(v) \quad (41)$$

which can be equivalently written as a complementarity problem

$$\begin{cases} v = \lambda_2 - v_z \\ y_1 = v_z - v, \\ y_2 = i + \lambda_1 \end{cases} \quad \text{and} \quad 0 \leq \begin{pmatrix} y_1 \\ y_2 \end{pmatrix} \perp \begin{pmatrix} \lambda_1 \\ \lambda_2 \end{pmatrix} \geq 0. \quad (42)$$

2) Hybrid Single-Valued Ideal Model in VERILOG/ELDO:

Using a Netlist and a Verilog description of the relation (43) to represent the couple of Zener diodes, a hybrid single-valued model reads as

$$v = \begin{cases} v_z & \text{if } i < 0 \\ 0 & \text{if } i = 0 \\ -v_z & \text{if } i > 0. \end{cases} \quad (43)$$

B. Smooth Model Using Hyperbolic Tangent Function in ELDO

Another approach consists in using the hyperbolic tangent function to approximate the multivalued components D_1 and D_2 . The relation between v and i is $v = -v_z \tanh(av)$. The coefficient a is chosen sufficiently large in order to neglect the influence of the regularization. We chose the value 10^5 to simulate the circuit using ELDO.

C. Simulation and Comparisons

The initial conditions are chosen as $i(0) = 0$ A, $v_{cap}(0) = -10$ V and the value of v_z is 0.5 V. The simulation using the linear complementarity problem is successfully achieved with SICONOS. The result is shown in Fig. 7(a). This electrical circuit dissipates some energy, so v_{cap} oscillates with a decreasing amplitude up to a threshold value v_z . After the first event at $t = t_b$, the current i vanishes and the voltage through the capacitor v_{cap} is stabilized to a nonzero value, equal to v through the double Zener diodes component. Note that this equilibrium point is located in the multivalued part of the characteristic.

Such a behavior exactly corresponds to the dynamics (40–41), for which the segment $\{(i, v_{cap}) \mid i = 0, -v_z \leq v_{cap} \leq v_z\}$ is an attractive sliding surface, attained in a finite time. When

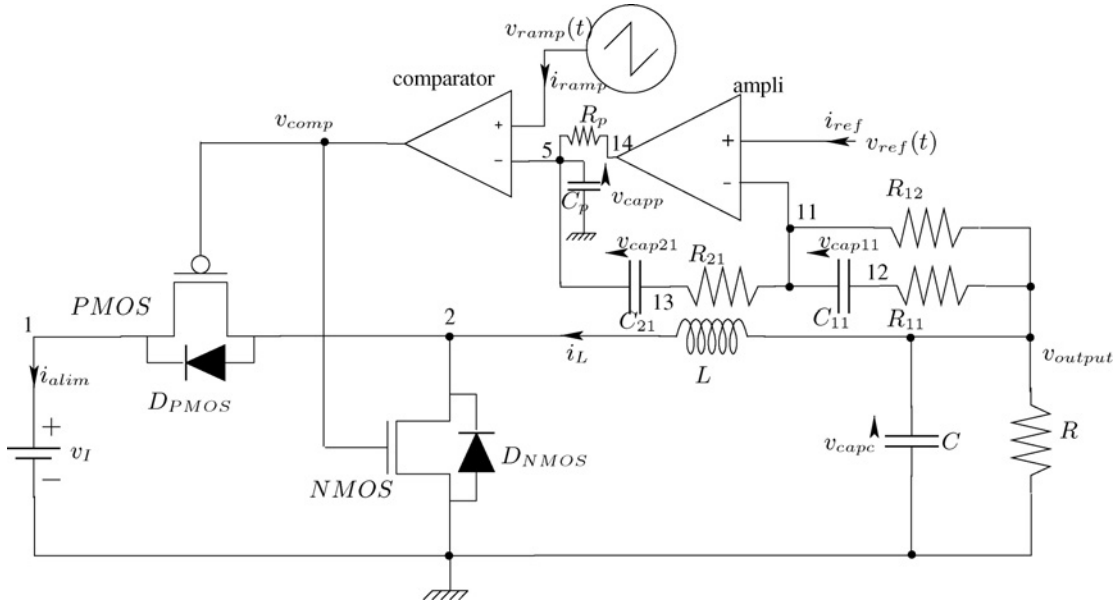


Fig. 8. Buck converter.

$i = 0$, it follows from (41) that $v_{cap} \in [-v_z, v_z]$. See [5] for more details.

Fig. 7(a) shows also the ELDO simulation using the Netlist and the VERILOG relation (43). In this case, the simulation is correctly done until t_b . At the first event at time t_b , the simulation cannot be continued because the equilibrium point of the circuit is not handled by the model.

The simulation using the hyperbolic function has been made using ELDO. We focus our attention on the difference due to the regularization of the multivalued model. The Fig. 7(b) zooms on the moment where the current vanishes. At this instant, the circuit is equivalent to an RLC circuit where the value of R is the coefficient of the tangent to the hyperbolic curve a . Note that using a coefficient a larger than 10^5 leads to an artificial v oscillation around the value of v_{cap} . The conclusion is that we cannot expect to observe the convergence toward an ideal behavior with such a regularization.

V. RESULTS ON THE BUCK CONVERTER

We conclude the numerical experiments with the less academic example of a buck converter described in Fig. 8. The components are modeled with linear, or piecewise-smooth, or set-valued relations yielding a nonsmooth dynamical system of the linear time invariant complementarity systems class. The features of the models are given thereafter.

A. Nonsmooth MOSFET Transistors

Following [34], let us consider the Sah model of the nMOS static characteristic:

$$i_{ds} = \frac{K}{2} \cdot (f(v_g - v_s - v_t) - f(v_g - v_d - v_t)) \quad (44)$$

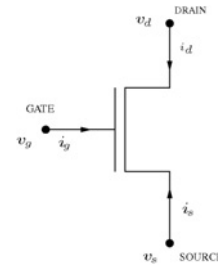


Fig. 9. nMOS transistor symbol.

with $K = \mu \frac{\epsilon_{OX} W}{t_{OX} L}$, μ mobility of majority carriers, W and L channel width and length, ϵ_{OX} the permittivity of the silicon oxide of thickness t_{OX} . The voltage v_t is the threshold voltage depending on the technology. The notation for the currents and the potentials at the ports of the nMOS is as in Fig. 9. The function $f: \mathbb{R} \rightarrow \mathbb{R}$ in (44) is defined as

$$f(x) = \begin{cases} 0 & \text{if } x < 0 \\ x^2 & \text{if } x \geq 0. \end{cases} \quad (45)$$

1) *Piecewise-Linear Model*: The piecewise and quadratic nature of this function is approximated by the following $s + 2$ segments piecewise-linear function [34]:

$$f_{pwl}(x) = \alpha_i x + \beta_i, \text{ for } a_i \leq x \leq a_{i+1}, \quad i = -1, \dots, s + 1 \quad (46)$$

with $a_{-1} = -\infty$ and $a_{s+1} = +\infty$. The complete model of the piecewise-linear nMOS transistor with $s + 2$ segments in (46) can be recast under the following mixed linear

complementarity form:

$$\begin{aligned}
 y(t) &= \left[\underbrace{\begin{matrix} 0 & \dots & 0 \\ -b & \dots & -b \end{matrix}}_{\times s+1} \quad \underbrace{\begin{matrix} -b & \dots & -b \\ 0 & \dots & 0 \end{matrix}}_{\times s+1} \right]^T v(t) + \lambda(t) \\
 &\quad + \left[h_1 \quad \dots \quad h_{s-1} \quad h_1 \quad \dots \quad h_{s-1} \right]^T \\
 0 &= I_3 i(t) + \left[\begin{matrix} -c_1 & \dots & -c_{s-1} & c_1 & \dots & c_{s-1} \\ 0 & 0 & 0 & 0 & 0 & 0 \\ c_1 & \dots & c_{s-1} & -c_1 & \dots & -c_{s-1} \end{matrix} \right] \lambda(t) \\
 0 &\leq y(t) \perp \lambda(t) \geq 0 \\
 v(t) &= \begin{bmatrix} v_{gd}(t) = v_g(t) - v_d(t) \\ v_{gs}(t) = v_g(t) - v_s(t) \end{bmatrix}, \quad i(t) = \begin{bmatrix} i_d(t) \\ i_g(t) \\ i_s(t) \end{bmatrix}.
 \end{aligned} \tag{47}$$

The parameters are given as follows: $b = \frac{K}{2}$, $h_i = b(v_i + a_i)$, $i = 1 \dots s$. The values c_i are computed from the linear approximation in (46). Using some basic convex analysis, one obtains the compact formulation of (47)

$$\begin{cases} -y(t) \in N_K(\lambda(t)) \\ y(t) = Bu(t) + \lambda(t) + h(t) \\ 0 = i(t) + C\lambda(t) \end{cases} \tag{48}$$

with $K = (\mathbb{R}_+)^{2(s+1)}$. In the case of the MOSFET transistor, the inclusion is an equality as expected since its piecewise-linear characteristic is single valued. The pMOS transistor is represented in the same way, changing the values of h_i , $i(t)$ to $-i(t)$ and b to $-b$.

Contrarily to the other models of components, the complementarity variables y and λ have no direct physical meaning. They are just slackness variables that permit us to express the presence of the operating point in the different segments of the model. For more details on the construction and the calibration of such a model, we refer to [34].

Remark 3: The piecewise-linear model in (46) has $s + 2$ segments. Multiple choices are possible in order to adjust the number of slack variables and consequently the size of the OSNSP-MLCP to be solved at each step with respect to the accuracy. In practice, one should therefore be very careful about choosing a reasonable piecewise-linear approximation of the devices so that the MLCP size does not increase too much.

2) *Piecewise-Nonlinear Model:* The model (44) can be modeled using the piecewise-nonlinear model (49). This leads to a nonlinear MCP

$$\begin{cases} i_{ds} = \frac{K}{2}(\lambda_4(v_g - v_s - v_t)^2 - \lambda_2(v_g - v_d - v_t)^2) \\ y_1 = 1 - \lambda_2 \\ y_2 = v_t - v_g + v_d + \lambda_1 \\ y_3 = 1 - \lambda_4 \\ y_4 = v_t - v_g + v_s + \lambda_3 \end{cases} \tag{49}$$

and $0 \leq y \perp \lambda \geq 0$. More generally, within the MCP framework, the models are not reduced to be piecewise-linear, but any piecewise-smooth function can be treated.

B. Parameters and Models Used for the Simulation

1) *Power MOSFETs pMOS/nMOS:* they are described as an assembly of a piecewise-linear current source $i_{ds} = f(v_{gs}, v_{ds})$, and the intrinsic diode (DpMOS and DnMOS) with an ideal characteristic. The capacitances were not taken into account. The diodes residual voltage is 0.8V. The MOSFETs transconductance K was set to $10 \text{ A} \cdot \text{V}^{-2}$ and their threshold voltage to respectively $v_t = -2 \text{ V}$ for the pMOS and $v_t = 2 \text{ V}$ for the nMOS. One can notice that the sum of their absolute values largely exceeds the supply voltage $v_i = 3 \text{ V}$, thus providing nonoverlapping conduction times. The other physical parameters are chosen as follows: $\mu = 750 \text{ cm}^2 \cdot \text{V}^{-1} \cdot \text{s}^{-1}$ for a nMOS and $\mu = 250 \text{ cm}^2 \cdot \text{V}^{-1} \cdot \text{s}^{-1}$ for a pMOS, $\epsilon_{OX} = \epsilon_r \text{ SiO}_2 \cdot \epsilon_0$ with $\epsilon_r \text{ SiO}_2 \approx 3.9$, $t_{OX} \approx 4 \text{ nm}$ $W = 130 \text{ nm}$ $L = 180 \text{ nm}$.

The piecewise-linear model we choose has 6 segments ($s = 4$) given by the following data: $c_1 = 0.09$, $c_2 = 0.2238$, $c_3 = 0.4666$, $c_4 = 1.1605$, $c_5 = 2.8863$, $a_1 = 0$, $a_2 = 0.1$, $a_3 = 0.2487$, $a_4 = 0.6182$, and $a_5 = 1.5383$. The relative error between $f(\cdot)$ and $f_{\text{pwl}}(\cdot)$ is kept below 0.1 for $0.1 \leq x < 3.82$. The absolute error is less than $2 \cdot 10^{-3}$ for $0 \leq x < 0.1$ and 0 for negative x . In practice, the values of v_g , v_s , v_d , v_t in logic integrated circuits allow a good approximation of $f(\cdot)$ by $f_{\text{pwl}}(\cdot)$.

2) *Other Components:*

a) *Compensator Amplifier:* It is modeled as a 10^5 gain and an output low-pass filter with a cutoff frequency of 30 MHz, composed of $R_p = 1 \Omega$ and $C_p = 5.3 \text{ nF}$.

b) *Comparator:* It is modeled as a piecewise-linear function whose value is 0 if $x < -\epsilon \text{ V}$ and 3 if $x > \epsilon \text{ V}$, with $\epsilon = 0.15$.

c) *Ramp Voltage:* The frequency is 600 kHz and the bounds are 0 and $0.75v_i = 2.25 \text{ V}$. The rise time is 1.655 ns and the fall time is 10 ns.

d) *Standard Values for Other Components:* $v_i = 3 \text{ V}$, $L = 10 \mu \text{ H}$, $C = 22 \mu \text{ F}$, $R_{\text{load}} = 10 \Omega$, $R_{11} = 15.58 \text{ k}\Omega$, $R_{12} = 227.8 \text{ k}\Omega$, $R_{21} = 5.613 \text{ M}\Omega$, $C_{11} = 20 \text{ pF}$, $C_{21} = 1.9 \text{ pF}$.

The reference voltage V_{ref} rises from 0 to 1.8 V in 0.1 ms at the beginning of the simulation. The output voltage v_{output} is regulated to track the reference voltage v_{ref} when v_i or v_{ref} or the load current vary. The error voltage v_{error} is a filtered value of the difference between v_{output} and v_{ref} . This voltage signal is converted into a time length thanks to a comparison with the periodic ramp signal. The comparator drives the pMOS transistor which in turn provides more or less charge to the output depending on the error level. The operation of a buck converter involves both a relatively slow dynamics when the switching elements (MOS and diodes) are keeping their conducting state, and a fast dynamics when the states change. The orders of magnitude are 50 ps for some switching details, 1 $\mu \text{ s}$ for a slow variation period and 100 $\mu \text{ s}$ at least for a settling period of the whole circuit requiring a simulation.

C. Dynamical Equations

The nonsmooth DAE has been generated using the automatic circuit equation formulation described in

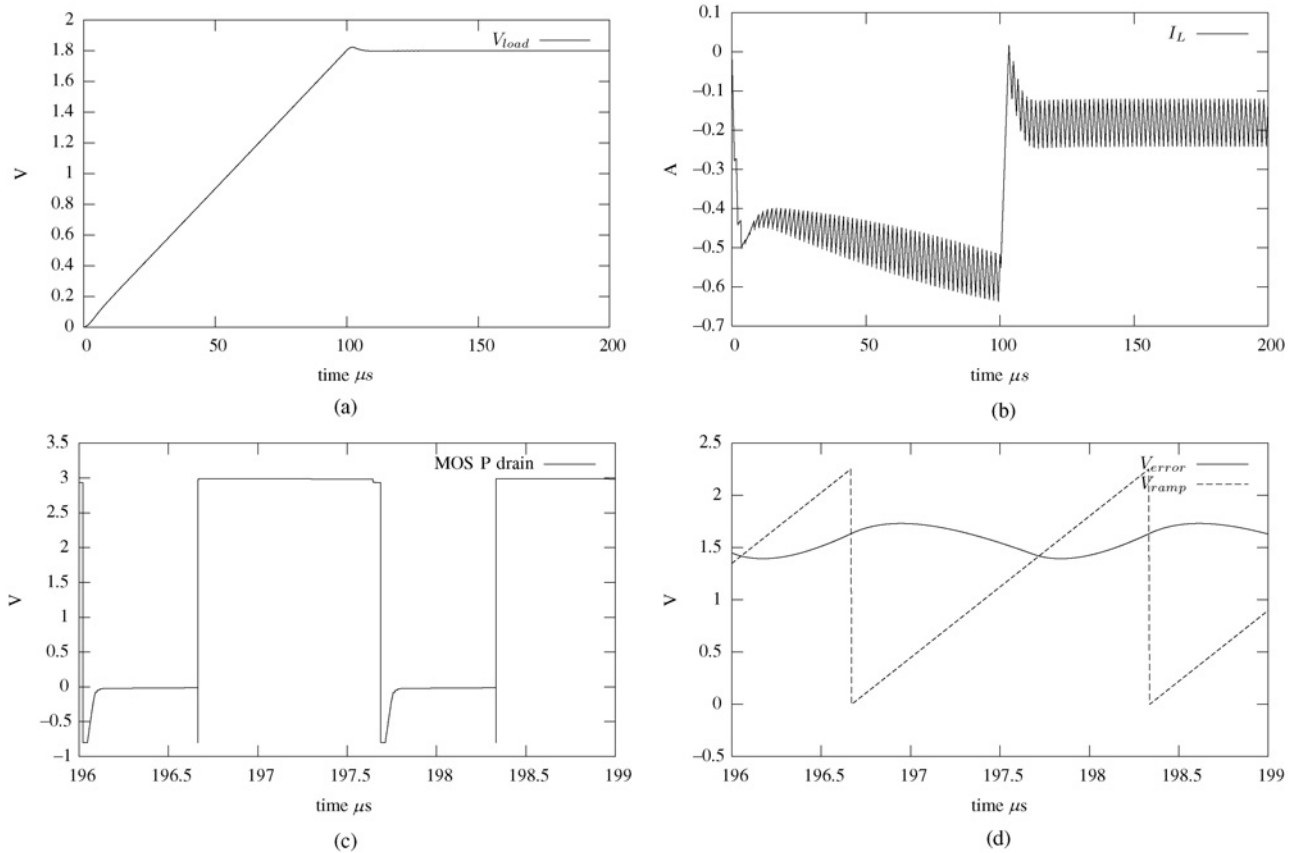


Fig. 10. SICONOS buck simulation using standard parameters. (a) v_{load} . (b) i_L . (c) pMOS drain potential. (d) v_{ramp} and v_{error} .

Section II-B2. It leads to a dynamical system described in (21) composed of five dynamical equations and 12 algebraic equations. The unknowns are $x = (v_{capp} v_{cap21} v_{cap11} v_{cap} i_L)^T$ and $z = (v_1 v_2 v_{comp} v_{ramp} v_{ref} v_{11} v_{14} i_{ref} i_{ramp} i_{alim} i_{ampli})^T$, where the unknowns are depicted in Fig. 8. The dimension of the inclusion rule is 24.

D. Simulation With SICONOS

The start-up of the converter was simulated thanks to SICONOS. As initial conditions, all state variables are zeroed. The detailed analysis of the switching events requires to use a time-step as small as 50 ps. The simulations are carried with a fixed time-step, $4 \cdot 10^6$ steps are then computed for the 200 μ s long settling of the output voltage. The OSNSP solvers are PATH with a convergence tolerance of 10^{-7} , and a semi-smooth Newton method based on the Fischer–Burmeister reformulation [20] that is our own implementation using a convergence tolerance of 10^{-12} . The overall result is shown on the Fig. 10.

Simulation time: The CPU time required to achieve the simulation is 60 s on a Pentium IV processor clocked at 3 GHz. It includes 19 s in the MLCP solvers, and 40 s in matrices products. The time to export the resulting data is not included.

- 1) Fig. 10(a) is the output potential, following the ramp v_{ref} .
- 2) Fig. 10(b) is the current through the inductor. Until 0.0001 s, i_L is loading the capacitor C. After 0.0001 s, i_L has to keep the capacitor charge constant.

3) Fig. 10(c) zooms on the pMOS drain potential with standard parameters.

4) Fig. 10(d) zooms on the v_{error} and v_{ramp} voltages.

The simulation has been tested with many parameters values. The robustness of the nonsmooth modeling and solving algorithms enables one to perform with the same CPU time the simulation of such cases. All the SICONOS simulations presented in this paper have been obtained in one-shot from the dynamical equations automatically generated from the Netlist, without any further parameter tuning.

In [3], several simulations are made with some parameters values that exhibit sliding mode trajectories. Furthermore, some comparisons with the models and the simulations of ELDO, NGSPICE, and PLECS can be found in [3].³ Simulations and comparisons are very encouraging in terms of the computational efficiency as well as the robustness and the accuracy of the simulation.

E. Simulation Using the Piecewise-Nonlinear Model (49)

The accuracy of the piecewise-linear model in (46) as function of the number of segments is given in Fig. 11. It consists in comparing the simulations to a reference simulation using the piecewise-nonlinear model (49). Fig. 11 shows the average and the maximum error of the state vector as function of the number of segments. Although the convergence is achieved, the number of segments, when it is small, can have

³A hybrid simulator developed by Plexim <http://www.plexim.com/>.

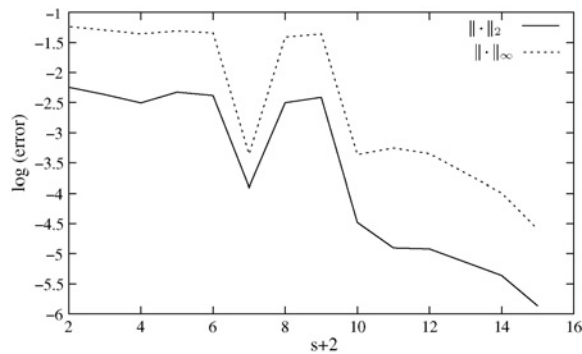


Fig. 11. Global error versus the number of segments.

an important effect on the behavior of the component and the convergence is not monotone. If the accuracy is an important criteria, the piecewise-nonlinear model (49) has to be used.

VI. CONCLUSION

In this paper, we have presented numerical simulations of switched circuits obtained with a suitable time-stepping implicit method, named Moreau's time-stepping algorithm. This method is based on the NSDS modeling approach, and relies heavily on complementarity problems (equivalently, inclusions into normal cones) solvers. The advantages of such a method are that it allows one to:

- 1) avoid computing the dynamics changes due to topology variations, since the circuits are treated as a global system with a fixed state dimension; modes transitions are taken care of by the complementarity problems solvers, which practically are polynomial in time;
- 2) simulate circuits with very large number of events without slowing down too much the simulation;
- 3) avoid regularization and consequently stiff systems of ODEs;
- 4) accurately simulate sliding mode trajectories without spurious oscillations around the switching surface.

Among the other great interests for such an approach that have not been developed in this article, we can cite:

- 5) the accurate calculation of the steady state of the system (see [10]);
- 6) the computation of the state jumps (initial jumps due to inconsistent states, or in the course of the integration), see simple circuits examples in [4].

The major drawback of the used method is its low order, so that its accuracy may be less good on smooth portions of the trajectories. In this paper, it is first shown that Moreau's time-stepping scheme allows one to integrate an academic example on which Newton–Raphson's method fails. Then, it is shown on a simple circuit that the scheme allows to perfectly handle sliding mode trajectories. Finally, the buck converter system is simulated. The simulations have been led with the SICONOS software package of the INRIA, an open source platform dedicated to nonsmooth multivalued dynamical systems.

ACKNOWLEDGMENT

The authors would like to thank P. Denoyelle for his contribution in the earlier version of this paper. They are also

grateful to M. Ferris at University of Wisconsin, Madison, for providing them with the PATH solver.

REFERENCES

- [1] V. Acary, "Toward higher order event-capturing schemes and adaptive time-step strategies for nonsmooth multibody systems," INRIA, St. Ismier Cedex, France, Tech. Rep. 7151, 2009.
- [2] V. Acary, O. Bonnefon, and B. Brogliato, "Improved circuit simulator," Patent 09/02605, May 2009.
- [3] V. Acary, O. Bonnefon, and B. Brogliato, "The nonsmooth dynamical systems approach for the analog simulation of switched circuits within the SICONOS framework," INRIA, St. Ismier Cedex, France, Tech. Rep. 7061, 2009.
- [4] V. Acary and B. Brogliato, *Numerical Methods for Nonsmooth Dynamical Systems: Applications in Mechanics and Electronics* (Lecture Notes in Applied and Computational Mechanics Series), vol. 35. Berlin, Germany: Springer-Verlag, 2008.
- [5] V. Acary and B. Brogliato, "Implicit Euler numerical scheme and chattering-free implementation of sliding mode systems," *Syst. Control Lett.*, vol. 59, no. 5, pp. 284–293, 2010.
- [6] V. Acary, B. Brogliato, and D. Goeleven, "Higher order Moreau's sweeping process: Mathematical formulation and numerical simulation," *Math. Program. A*, vol. 113, no. 1, pp. 133–217, 2008.
- [7] V. Acary and F. P erignon, "An introduction to SICONOS," INRIA, St. Ismier Cedex, France, Tech. Rep. TR-0340, 2007 [Online]. Available: <http://hal.inria.fr/inria-00162911/en/>
- [8] V. Acary and F. P erignon, "SICONOS: A software platform for modeling, simulation, analysis and control of nonsmooth dynamical systems," *Simulat. News Eur.*, vol. 17, nos. 3–4, pp. 19–26, Dec. 2007.
- [9] K. Addi, S. Adly, B. Brogliato, and D. Goeleven, "A method using the approach of Moreau and Panagiotopoulos for the mathematical formulation of nonregular circuits in electronics," *Nonlinear Anal.: Hybrid Syst.*, vol. 1, no. 1, pp. 30–43, Mar. 2007.
- [10] K. Addi, B. Brogliato, and D. Goeleven, "A qualitative mathematical analysis of a class of linear variational inequalities via semi-complementarity problems: Applications in electronics," *Math. Program. A*, 2008, to be published.
- [11] S. B achle and F. Ebert, "Element-based topological index reduction for differential-algebraic equations in circuit simulation," *Inst. f. Math., TU Berlin, Germany, Tech. Rep. Preprint 05-246 (Matheon)*, 2005.
- [12] S. B achle and F. Ebert, "Graph theoretical algorithms for index reduction in circuit simulation," *Inst. f. Math., TU Berlin, Germany, Tech. Rep. Preprint 05-245 (Matheon)*, 2005.
- [13] C. Batlle, E. Fossas, and A. Miralles, "Generalized discontinuous conduction modes in the complementarity formalism," *IEEE Trans. Circuits Syst. II: Exp. Briefs*, vol. 52, no. 8, pp. 447–451, Aug. 2005.
- [14] S. Billups, S. Dirkse, and M. Ferris, "A comparison of large scale mixed complementarity problem solvers," *Comput. Optim. Applicat.*, vol. 7, pp. 3–25, 1997.
- [15] D. Birolek and J. Dobes, "Computer simulation of continuous-time and switched circuits: Limitations of SPICE-family programs and pending issues," in *Proc. 17th Int. Conf. Radioelektron.*, Apr. 24–25, 2007, pp. 1–11.
- [16] M. K. Camlibel, W. Heemels, and J. Schumacher, "Consistency of a time-stepping method for a class of piecewise-linear networks," *IEEE Trans. Circuits Syst. I*, vol. 49, no. 3, pp. 349–357, Mar. 2002.
- [17] M. Cao and M. Ferris, "A pivotal method for affine variational inequalities," *Math. Oper. Res.*, vol. 21, no. 1, pp. 44–64, 1996.
- [18] H. Chung and A. Ioinovici, "Fast computer aided simulation of switching power regulators based on progressive analysis of the switches' state," *IEEE Trans. Power Electron.*, vol. 9, no. 2, pp. 206–212, Mar. 1994.
- [19] R. W. Cottle, J. Pang, and R. E. Stone, *The Linear Complementarity Problem*. Boston, MA: Academic Press, Inc., 1992.
- [20] T. DeLuca, F. Facchinei, and C. Kanzow, "A semismooth equation approach to the solution of nonlinear complementarity problems," *Math. Program.*, vol. 75, no. 2, pp. 407–439, 1996.
- [21] P. Denoyelle and V. Acary, "The non-smooth approach applied to simulating integrated circuits and power electronics. Evolution of electronic circuit simulators toward fast-SPICE performance," INRIA, France, INRIA Res. Rep. 0321, 2006 [Online]. Available: <http://hal.inria.fr/docs/00/08/09/20/PDF/RT-0321.pdf>
- [22] S. P. Dirkse and M. C. Ferris, "The PATH solver: A non-monotone stabilization scheme for mixed complementarity problems," *Optim. Methods Softw.*, vol. 5, no. 2, pp. 123–156, 1995.

- [23] H. Elmqvist, S. Mattsson, and M. Otter, "Object-oriented and hybrid modling in Modelica," *J. Eur. Syst. Automat.*, vol. 35, no. 4, pp. 395–404, 2001.
- [24] O. Enge and P. Maisser, "Modeling electromechanical systems with electrical switching components using the linear complementarity problem," *Multibody Syst. Dynam.*, vol. 13, no. 4, pp. 421–445, 2005.
- [25] F. Facchinei and J. S. Pang, *Finite-Dimensional Variational Inequalities and Complementarity Problems* (Springer Series in Operations Research), vols. I and II. New York: Springer-Verlag, 2003.
- [26] R. Frasca, M. Camlibel, I. Goknar, and F. Vasca, "State jump rules in linear passive networks with ideal switches," in *Proc. IEEE ISCAS*, May 2008, pp. 540–543.
- [27] M. Fukushima, "Equivalent differentiable optimization problems and descent methods for asymmetric variational inequality problems," *Mathematical Programming*, vol. 53, nos. 1–3, pp. 99–110, 1992.
- [28] Z. Galias and X. Yu, "Complex discretization behaviors of a simple sliding-mode control system," *IEEE Trans. Circuits Syst. II: Exp. Briefs*, vol. 53, no. 8, pp. 652–656, Aug. 2006.
- [29] C. Glocker, "Models of non-smooth switches in electrical systems," *Int. J. Circuit Theory Applicat.*, vol. 33, no. 3, pp. 205–234, 2005.
- [30] D. Goeleven, "Existence and uniqueness for a linear mixed variational inequality arising in electrical circuits with transistors," *J. Optim. Theory Applicat.*, vol. 138, no. 3, pp. 397–406, Sep. 2008.
- [31] J. Hiriart-Urruty and C. Lemaréchal, *Convex Analysis and Minimization Algorithms*, vols. I and II. Heidelberg, Germany: Springer-Verlag, 1993.
- [32] M. Jean, "The non-smooth contact dynamics method," *Comput. Methods Appl. Mech. Eng.*, vol. 177, nos. 3–4, pp. 235–257, 1999.
- [33] S. Kang and L. Chua, "A global representation of multidimensional piecewise-linear functions with linear partitions," *IEEE Trans. Circuits Syst.*, vol. 25, no. 11, pp. 938–940, Nov. 1978.
- [34] D. Leenaerts and W. Van Bokhoven, *Piecewise Linear Modeling and Analysis*. Norwell, MA: Kluwer, 1998.
- [35] D. Leenaerts, "On linear dynamic complementarity systems," *IEEE Trans. Circuits Systems: Fundam. Theory Applicat.*, vol. 46, no. 8, pp. 1022–1026, Aug. 1999.
- [36] P. Maffezzoni, L. Codecasa, and D. D'Amore, "Event-driven time-domain simulation of closed-loop switched circuits," *IEEE Trans. Comput.-Aided Design Integr. Circuits Syst.*, vol. 25, no. 11, pp. 2413–2426, Nov. 2006.
- [37] K. Mayaram, D. Lee, D. Moinian, and J. Roychowdhury, "Computer-aided circuit analysis tools for RFIC simulation: Algorithms, features, and limitations," *IEEE Trans. Circuits Syst. II: Analog Digital Signal Process.*, vol. 47, no. 4, pp. 274–286, Apr. 2000.
- [38] M. Moeller and C. Glocker, "Non-smooth modeling of electrical systems using the flux approach," *Nonlinear Dynam.*, vol. 50, nos. 1–2, pp. 273–295, 2007.
- [39] J. J. Moreau, "Evolution problem associated with a moving convex set in a Hilbert space," *J. Differential Eqs.*, vol. 26, no. 3, pp. 347–374, 1977.
- [40] J. J. Moreau, "Bounded variation in time," in *Topics in Nonsmooth Mechanics*, J. J. Moreau, P. D. Panagiotopoulos, and G. Strang, Eds. Basel, Switzerland: Birkhäuser, 1988, pp. 1–74.
- [41] J. J. Moreau, *Unilateral Contact and Dry Friction in Finite Freedom Dynamics* (CISM Courses and Lectures Series 302). Berlin, Germany: Springer-Verlag, 1988, ch. 1, pp. 1–82.
- [42] J. J. Moreau, "Numerical aspects of the sweeping process," *Comput. Methods Appl. Mech. Eng.*, vol. 177, nos. 3–4, pp. 329–349, 1999.
- [43] R. Rockafellar, *Convex Analysis*. Princeton, NJ: Princeton Univ. Press, 1970.
- [44] R. Sargent, "An efficient implementation of the Lemke algorithm and its extension to deal with upper and lower bounds," *Mathematical Programming Study*, vol. 7, pp. 36–54, 1978.
- [45] S. Stevens and P. Lin, "Analysis of piecewise-linear resistive networks using complementarity pivot theory," *IEEE Trans. Circuits Syst.*, vol. 28, no. 5, pp. 429–441, May 1981.
- [46] W. van Bokhoven and J. Jess, "Some new aspects of P and P_0 matrices and their application to networks with ideal diodes," in *Proc. IEEE Int. Symp. Circuits Syst.*, 1978, pp. 806–810.
- [47] L. Vandenberghe, B. De Moor, and J. Vandewalle, "The generalized linear complementarity problem applied to the complete analysis of resistive piecewise-linear circuits," *IEEE Int. Symp. Circuits Syst.*, vol. 36, no. 11, pp. 1382–1391, Nov. 1989.
- [48] F. Vasca, L. Iannelli, M. Camlibel, and R. Frasca, "A new perspective for modeling power electronics converters: Complementarity framework," *IEEE Trans. Power Electron.*, vol. 24, no. 2, pp. 456–468, Feb. 2009.
- [49] J. Vlach and A. Opal, "Modern CAD methods for analysis of switched networks," *IEEE Int. Symp. Circuits Syst. I: Fundam. Theory Applicat.*, vol. 44, no. 8, pp. 759–762, Aug. 1997.
- [50] J. Vlach, J. Wojciechowski, and A. Opal, "Analysis of nonlinear networks with inconsistent initial conditions," *IEEE Int. Symp. Circuits Syst. I: Fundam. Theory Applicat.*, vol. 42, no. 4, pp. 195–200, Apr. 1995.
- [51] F. Yuan and A. Opal, "Computer methods for switched circuits," *IEEE Int. Symp. Circuits Syst. I: Fundam. Theory Applicat.*, vol. 50, no. 8, pp. 1013–1024, Aug. 2003.
- [52] D. Zhu and P. Marcotte, "Modified descents methods for solving the monotone variational inequality problem," *Oper. Res. Lett.*, vol. 14, no. 2, pp. 111–120, 1993.
- [53] D. Zhu and P. Marcotte, "An extended descent framework for monotone variational inequalities," *J. Optim. Theory Applicat.*, vol. 80, no. 2, pp. 349–366, 1994.



Vincent Acary was born in 1973 in Laval, France. He graduated from the Ecole Centrale de Marseille, Marseille Cedex, France, in 1997, and received the Ph.D. degree in mechanical engineering from the Aix-Marseille II University, Aix-en-Provence Cedex, France, in 2001.

He is currently a Research Fellow with INRIA Grenoble Rhône-Alpes, St. Ismier Cedex, France. He co-authored a monograph with B. Brogliato titled, *Numerical Methods for Nonsmooth Dynamical Systems* (Berlin, Germany: Springer, LNACM series

vol. 35, 2008). His current research interests include nonsmooth dynamical systems with applications in mechanics, circuits, optimal control, and variable-structure systems.



Olivier Bonnefon was born in 1973 in Saintes, France. He graduated from the École Nationale Supérieure d'Informatique et de Mathématiques Appliquées de Grenoble, Grenoble, France.

He is currently a Research Engineer with INRIA Grenoble Rhône-Alpes, St. Ismier Cedex, France. His current research interests include nonsmooth dynamical circuits (modeling and software aspects).



Bernard Brogliato was born in 1963 in Saint-Symphorien de Lay, France. He graduated from the Department of Mechanical Engineering, École Normale Supérieure de Cachan, Cachan, France, and received the Ph.D. degree in automatic control from the National Polytechnic Institute of Grenoble (INPG), Grenoble, France, in 1991.

He is currently with at INRIA Grenoble Rhône-Alpes, St. Ismier Cedex, France, as a Scientific Leader of the team BIPOP. He authored and co-authored four monographs: *Nonsmooth Mechanics* (Berlin, Germany: Springer, CCE Series, 2nd ed., 1999), *Dissipative Systems Analysis and Control* (Berlin, Germany: Springer, CCE Series, 2nd ed., 2007), *Numerical Methods for Nonsmooth Dynamical Systems* (Berlin, Germany: Springer, LNACM Series, vol. 35, 2008), *Nonsmooth Modeling and Simulation for Switched Circuits* (Berlin, Germany: Springer, LNEE Series, 2010). His current research interests include nonsmooth dynamical systems and dissipative systems (modeling, control, analysis), with applications in mechanics, circuits, optimal control, and variable-structure systems.